82661-50-5; $[CpMo(CO)_3]_2(S_2O_4)$, 98126-18-2; $Na[CpMo(CO)_3]$, 12107-35-6; $[CpMo(CO)_3]_2$, 12091-64-4; $[CpW(CO)_3]_2$, 12091-65-5; $CpW(CO)_2[P(OPh)_3]H$, 31811-84-4; $Cp^*Mo(CO)_2[P(OPh)_3]H$, 98105-21-6; CpW(CO)2$(PBu_3)H$, 65437-11-8; $CpW(CO)_2(PPh_2Me)H$, 61300-90-1; $[CpW(CO)_3]_2(\mu\text{-}S)$, 92468-48-9; $[Cp^*W(CO)_2(\mu\text{-}S{\bullet}SO_2)]_2$, 94024-81-4; $Cp^*{}_2W_2(CO)_2S_3$, 82167-38-2; $Mo(CO)_3(CH_3CN)_3$, 15038-48-9; $[CpW(CO)_3]_2(\mu\text{-}S{\bullet}SO_2)$, 94024-80-3; [CpMo(CO)3]2(μ-S), 94024-83-6; SO_2, 7446-09-5; $S^{18}O_2$, 24262-77-9.

Supplementary Material Available: Elemental analyses (Table Is), anisotropic thermal parameters (Tables IIs and IIIs), interatomic C–C distances and angles (Tables IVs and Vs), and structure factor amplitudes (Tables VIs and VIIs) (17 pages). Ordering information is given on any current masthead page.

(Trimethylphosphine)cobalt(I) Complexes. 4. Reaction with Acyclic Dienes and Crystal Structure of (Butadiene)tris(trimethylphosphine)cobalt(I) Tetraphenylborate

L. C. Ananias de Carvahlo,[1a,c] Yolande Pérès,[1a] Michèle Dartiguenave,*[1a] Yves Dartiguenave,[1a]
and André L. Beauchamp*[1b]

Laboratoire de Chimie de Coordination du CNRS, 31400 Toulouse, France, and the Département de Chimie, Université de Montréal, Montréal, Canada H3C 3V1

Received January 25, 1985

Reaction of $CoBr(PMe_3)_3$ with butadiene, isoprene, and 2,3-dimethylbutadiene in presence of $NaBPh_4$ yielded $[Co(diene)(PMe_3)_3]BPh_4$ complexes. The crystal structure of $[Co(\eta^4\text{-}C_4H_6)(PMe_3)_3]BPh_4$ has been determined by X-ray diffraction techniques. The complex crystallizes in the monoclinic system, $C2/c$, with $a = 46.71$ (2) Å, $b = 15.93$ (4) Å, $c = 34.21$ (2) Å, $\beta = 118.69$ (4)°, $Z = 24$, and $R = 0.083$ (5587 "observed" reflections). The structure consists of a perfectly ordered framework of BPh_4^- anions, in which large cavities are occupied by $[Co(\eta^4\text{-}C_4H_6)(PMe_3)_3]^+$ cations. In only one-third of these cavities are the cations ordered. Two different kinds of disorder are found for the remaining cations. In the ordered cations, cobalt is in a distorted square-pyramidal environment. One of the PMe_3 molecules is apical, whereas two PMe_3 molecules and the butadiene ligand occupy the basal sites. The difference between the apical (2.192 (5) Å) and basal (average 2.221 (4) Å) Co–P bond lengths is significant but small. The butadiene ligand is planar within 0.5σ, and its plane makes an angle of 84.5° to the basal plane. It is symmetrically coordinated and the cobalt atom is located 0.60 Å above the basal plane. In one of the disordered cations, two isomeric forms related by a 120° rotation of the butadiene ligand about the pseudo C_3 axis of the $Co(PMe_3)_3$ fragment are observed, suggesting the possibility of fluxionality in the crystal. Multinuclear NMR studies (187–295 K) show that in solution the $[Co(\eta^4\text{-}diene)(PMe_3)_3]BPh_4$ compounds do not exist as η^3-allyl complexes with σ-CH_2 ligand-to-cobalt interactions but retain the η^4-diene structure observed in the solid state.

Introduction

As part of our continuing research involving the chemistry of first-row d^8 nickel and cobalt complexes with trimethylphosphine, we recently reported the reaction of $CoBr(PMe_3)_3$ with ethylene and diphenylacetylene,[2] which gave rise to the new complexes $[Co(C_2H_4)(MeCN)(PMe_3)_3]BPh_4$, **1**, $[Co(C_2Ph_2)(MeCN)(PMe_3)_3]BPh_4$, **2**, and $[Co(C_2Ph_2)(PMe_3)_3]BPh_4$, **3**. They can be envisioned as constituted from the 14-electron $[Co(PMe_3)_3]^+$ fragment accepting four electrons (either from two 2-electron species like ethylene, diphenylacetylene, acetonitrile, etc. or from one 4-electron species like diphenylacetylene) in order to fill the metal coordination sphere and reach the 18-electron configuration.[3] Unfortunately, this interpretation gives little information on the nature of the bond between Co and the organic ligand. This aspect is of interest since such complexes possess a reduced Co(I) metal center which could induce internal oxidative addition and thus activate the organic ligand, giving rise to new chemical reactions.

In order to get more information, we are currently investigating the reactions of $CoBr(PMe_3)_3$ with other 4-electron donor ligands: conjugated and nonconjugated dienes. In the present study, the $[Co(\eta^4\text{-}diene)(PMe_3)_3]BPh_4$ complexes of butadiene (I), isoprene (II), and 2,3-dimethylbutadiene (III) were synthesized in good yields by reacting $CoBr(PMe_3)_3$ with the diene in presence of $NaBPh_4$.[4] Their behavior in solution was examined by means of ^1H, ^{13}C, and ^{31}P NMR. To our knowledge, there are no crystallographic data on Co(I) compounds of this type. The crystal structure of the butadiene complex $[Co(\eta^4\text{-}C_4H_6)(PMe_3)_3]BPh_4$ (I) is reported here.

Experimental Section

Procedure, Reagents, and Solvents. All operations were carried out under purified argon atmosphere in a conventional vacuum system or in a Jaram glovebox. The solvents were distilled before use, transferred under argon, and degassed in vacuum line. PMe_3 was prepared following an improved variation of Wolfsberger and Schmidbaur's method[5] and stored under argon.

---

[1] (a) Laboratoire de Chimie de Coordinatin du CNRS. (b) Université de Montréal. (c) On leave from the Department of Chemistry of the Universidade Federal de Minas Gerais.

[2] Capelle, B.; Beauchamp, A. L.; Dartiguenave, M.; Dartiguenave, Y.; Klein, H. F. *J. Am. Chem. Soc.* **1982**, *104*, 3891–3897. Capelle, B.; Beauchamp, A. L.; Dartiguenave, M.; Dartiguenave, Y. *J. Chem. Soc., Chem. Commun.* **1982**, 566–568; *J. Am. Chem. Soc.* **1983**, *105*, 4662–4670.

[3] Elian, M.; Hoffman, R. *Inorg. Chem.* **1975**, *14*, 1058–1076.

[4] These complexes have been first synthesized by reacting PR_3 on Co(II) salts in 2-propanol: Bressan, M.; Ettorre, R.; Rigo, P. *J. Organomet. Chem.* **1984**, *144*, 215–223.

0276-7333/85/2304-2021$01.50/0

$\text{CoBr(PMe}_3)_3$ was synthesized following Klein and Karsch.[6] The diolefins were commercially available. Isoprene and 2,3-dimethylbutadiene were used after filtration through neutral grade alumina and degassing.

Synthesis of the $[\text{Co}(\eta^4\text{-diene})(\text{PMe}_3)_3]\text{BPh}_4$ Complexes. The three complexes were prepared following the same procedure. A solution of $\text{CoBr(PMe}_3)_3$ (1.4 g, 3.8 mmol) in acetonitrile (10 mL) was cooled to −10 °C and purged with the diene. The color of the solution changed from green to yellow. Then, NaBPh_4 (1.3 g, 3.8 mmol) dissolved in 25 mL of methanol was added. Yellow crystals precipitated from the solution kept at −30 °C overnight; they were filtered, dried, and stored under argon. Anal. (butadiene) Calcd for $\text{CoP}_3\text{BC}_{37}\text{H}_{53}$: C, 67.28; H, 8.09; P, 14.07; Co, 8.92. Found: C, 66.82; H, 8.44; P, 13.31; Co, 9.08. Anal. (isoprene) Calcd for $\text{CoP}_3\text{BC}_{38}\text{H}_{55}$: C, 67.67; H, 8.22; P, 13.78; Co, 8.74; B, 1.60. Found: C, 67.51; H, 8.32; P, 13.34; Co, 8.64; B, 1.57. Anal. (dimethylbutadiene) Calcd for $\text{CoP}_3\text{BC}_{39}\text{H}_{57}$: C, 68.03; H, 8.34; P, 13.50; Co, 8.56; B, 1.57. Found: C, 67.63; H, 8.15; P, 13.35; Co, 8.21; B, 1.58.

NMR Experiments. Variable-temperature ^{1}H, ^{1}H{^{31}P}, ^{31}P, ^{31}P{^{1}H}, ^{13}C, and ^{13}C{^{1}H} FT NMR spectra were recorded at 250 MHz for ^{1}H, 101.27 MHz for ^{31}P, and 62.9 MHz for ^{13}C, using a Bruker WM-250 spectrometer equipped with a special probe for observing ^{1}H and decoupling ^{31}P. Field-frequency stabilization was achieved on an internal ^{2}D signal at 38.39 kG. SiMe_4 was used as external reference for ^{1}H and ^{13}C chemical shifts. For ^{31}P, H_3PO_4 (62.5%) in D_2O was used as reference. The NMR tubes were prepared in the glovebox, using $(\text{CD}_3)_2\text{CO}$ or CD_2Cl_2 as solvents.

Crystal data for $\text{C}_{37}\text{H}_{53}\text{BCoP}_3$: fw = 660.5 monoclinic, $C2/c$, $a = 46.71$ (2) Å, $b = 15.93$ (4) Å, $c = 34.21$ (2) Å, $\beta = 118.69$ (4)°, $Z = 24$, $V = 22330$ Å^3, $D_{\text{calcd}} = 1.178$ g cm^{-3}, λ(Mo K$\bar{\alpha}$) = 0.71067 Å, $t = 23$ °C, μ(Mo Kα) = 6.1 cm^{-1}, crystal dimenions 0.62 mm (100–$\bar{1}$00) × 0.55 m (001–00$\bar{1}$) × 0.68 mm (010–0$\bar{1}$0).

Crystallographic Measurements. Yellow crystals suitable for X-ray work were obtained directly from the reaction mixture. No visible damage occurred to the crystal during the short time needed to seal it in a Lindemann capillary filled with nitrogen. Precession and cone axis photographs showed $2/m$ Laue symmetry, and the systematic absences (hkl, $h + k \neq 2n$; $h0l$, $l \neq 2n$) were consistent with space groups Cc and $C2/c$.

The crystal was mounted on an Enraf-Nonius CAD4 diffractometer. Accurate cell parameters and intensity data were obtained following the procedure described previously.[7] The mean fluctuation of three standard reflections was ±1.7% during data collection. A total of 10436 hkl and $hk\bar{l}$ reflections were measured ($2\theta \leq 40°$). The data in the 40–42° range were also measured, but they were not retained owing to the very low proportion of reflections above background. A set of 5587 reflections with intensities $I > 3\sigma(I)$ was used to solve the structure. The Lorentz and polarization corrections were applied. A sample calculation showed that the transmission factor would lie in the narrow 0.65–0.73 range. Therefore, no absorption correction was applied.

Resolution of the Structure. The density, estimated from similar compounds, suggested that the asymmetric unit contained three BPh_4^- ions and three Co complex cations in space group $C2/c$, twice as many in space group Cc. The distribution of the normalized structure factors clearly favored the centric group, and the structure was determined in the $C2/c$ space group.

The heavy-atom method yielded the correct solution, but only after a tedious series of unsuccessful attempts to interpret the Patterson synthesis. The map contained a large number of strong peaks, but assignments could not be straightforwardly deduced from their heights. This was subsequently ascribed to the fact that two of the three independent Co atoms are involved in disorder or high thermal motion, so that their contributions were comparable to those of any of the ordered P atom. A difference Fourier (ΔF) map phased on one of the consistent sets of three Co atom positions eventually showed a reasonable distribution of P atoms around each metal. From this point on, structure factor and ΔF map calculations progressively revealed most non-hydrogen atoms, namely, the three nonequivalent BPh_4^- ions and, for cation 1, the butadiene and the PMe_3 carbon atoms. No consistent pattern emerged at this stage for the butadiene molecules in cations 2 and 3.

The known portion of the structure was isotropically refined on $|F_o|$ by full-matrix least squares. Weights based on counting statistics[7] were applied. Convergence was reached for $R = ||F_o| - |F_c||/\sum|F_o| = 0.176$ and $R_w = [\sum w(|F_o| - |F_c|)^2/\sum w|F_o|^2]^{1/2} = 0.199$. From the new ΔF map, it became clear that the surroundings of Co(2) and Co(3) could not be described by an ordered model. However, there was no evidence for disorder in the BPh_4^- ions or in cation 1. In cation 2, two of the P atoms had thermal motion much greater than the other, and there was a pair of strong peaks too close to correspond to atoms simultaneously present within the same molecule. Thus, it was concluded that cation 2 was involved in a twofold disorder, with two phosphines occupying resolved positions and the third phosphine being common to both individuals. All the methyl carbon (or half-carbon) atoms were found for each of these P positions. As for the butadiene group, C(5) and C(6) occupied the same positions in both individuals. The third carbon atom was found in two close, but resolved, positions (C(7A) and C(7B)), whereas the positions for the terminal carbon atom (C(8A) and C(8B)) were close to those of P(24) and P(22), respectively, in the other individual. Therefore, C(8A) and C(8B) were fixed at the positions estimated by interpolation on the ΔF map, with $B = 10$ Å^2.

In cation 3, all P atoms had high thermal motion, but none of them was split into resolved components. All the attached methyl carbon atoms were identified, and they also had, as expected, high thermal motion. Five peaks remained around Co(3). They were attributed to the overlapping butadiene fragments. They were grouped into two sets defining a reasonable butadiene molecules, three atoms being common to both individuals.

For the rest of the interpretation, occupancy factors of 0.50 were arbitrarily assigned to the disordered components and no attempts were made to refine these parameters. Isotropic refinement converged to $R = 0.141$ and $R_w = 0.167$. The phenyl hydrogen atoms were positioned at ideal positions (sp^2 hybridization, C–H = 0.95 Å, $B = 6.0$ Å^2). Their parameters were not refined, but their coordinates were recalculated after each least-squares cycle. The hydrogen atoms in the phosphines or butadiene molecules were not found. The final steps were carried out by block-diagonal least squares. Anisotropic temperature factors were refined for all Co, P, and B atoms, as well as for the ordered C atoms. The final discrepancy factors were $R = 0.083$ and $R_w = 0.095$. The goodness-of-fit ratio was 2.37. The fractional coordinates are listed in Table I. The list of temperature factors and of structure factors are part of the supplementary material.

The scattering curves and anomalous dispersion coefficients of Co and P were from standard sources.[8] The programs used are listed elsewhere.[9]

Results and Discussion

Crystal Structure of $[\text{Co}(\eta^4\text{-C}_4\text{H}_6)(\text{PMe}_3)_3]\text{BPh}_4$. Crystals of $[\text{Co}(\eta^4\text{-C}_4\text{H}_6)(\text{PMe}_3)_3]\text{BPh}_4$ contain discrete $[\text{Co}(\eta^4\text{-C}_4\text{H}_6)(\text{PMe}_3)_3]^+$ cations and tetraphenylborate anions. Figure 1 shows a layer of alternating cations and anions, parallel to the cell ac plane. The adjacent layers are displaced by $a/2 + b/2$ (C centering), which brings two extra BPh_4^- ions, one above and one below, near any complex cation. The anions are rigorously ordered and they may be regarded as the framework of the crystal. The large cavities surrounded by six anions are filled by complex cations. In only one third of these cavities are the $[\text{Co}(\eta^4\text{-C}_4\text{H}_6)(\text{PMe}_3)_3]^+$ ions ordered (type 1). The disorder found for cations of type 2 and 3 is examined in detail below.

---

(5) Wolfsberger, W.; Schmidbaur, R. *Synth. Inorg. Metal-Org. Chem.* **1974**, *4*, 149–156.

(6) Klein, H. F.; Karsch, H. H. *Inorg. Chem.* **1975**, *14*, 473–477.

(7) Bélanger-Gariépy, F.; Beauchamp, A. L. *J. Am. Chem. Soc.* **1980**, *102*, 3461–3464.

(8) Cromer, D. T.; Waber, J. T. *Acta Crystallogr.* **1965**, *18*, 104–109. Stewart, R. F.; Davidson, E. R.; Simpson, W. T. *J. Chem. Phys.* **1965**, *42*, 3175–3187. Cromer, D. T. *Acta Crystallogr.* **1965**, *18*, 17–23.

(9) Authier-Martin, M.; Beauchamp, A. L. *Can. J. Chem.* **1977**, *55*, 1213–1217.

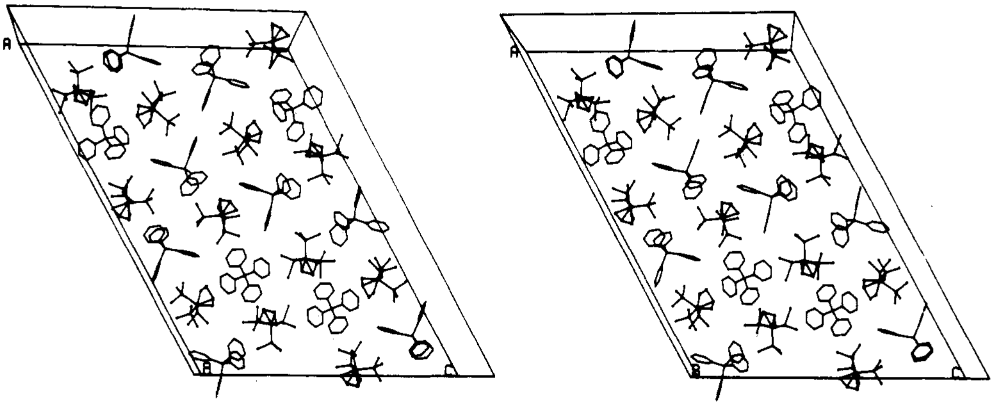

Figure 1. Stereoview of a layer of alternating $[Co(\eta^4\text{-}C_4H_6)(PMe_3)_3]^+$ and BPh_4^- ions down the b axis. The layers above and below are shifted by a/2 + b/2, bringing two extra BPh_4^- ions around any complex cation. Two-thirds of the cations are disordered. The Co complex cations and BPh_4^- anions are aligned along the *a* axis in the following order (from top to bottom): Co(3), $1 - x, y, -^3/_2 - z$); B(2), $(1 - x, y, ^1/_2 - z)$; Co(1), (x, y, z); B(1), (x, y, z); Co(2), $(x, 1 - y, -^1/_2 + z)$; B(3), (x, y, z).

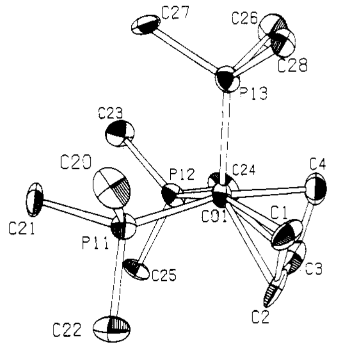

Figure 2. ORTEP drawing of the $[Co(\eta^4\text{-}C_4H_6)(PMe_3)_3]^+$ ion (type 1). Ellipsoids correspond to 30% probability.

Cation 1. The eight cations of this type in the cell are perfectly ordered. The interatomic distances are listed in Table II and bond angles in Table III. These values are not biased by overlapping images, and they can be used to discuss the structural features of the Co(I) complex. This species is best described as a distorted square pyramid (Figure 2) with P(13) occupying the axial site. P(11) and P(12) occupy two cis basal sites and the two double bonds of butadiene span the remaining basal sites. This description yields an 18-electron configuration for the complex, as was observed for ethylene and diphenylacetylene cobalt compounds.[2]

The Co–P distances compare well with those reported for (tertiary phosphine)metal complexes. The apical Co–P(13) bond (2.192 (5) Å) seems to be shorter than the basal ones (average 2.221 (4) Å), but the difference is barely significant. Comparisons are made in Table IV between structural parameters of this complex and those of the d^6 $RuCl_2(PPh_3)_3$ molecule[10] and other d^8 square-pyramidal Fe(0), Co(I), and Ni(II) compounds. The crystallographic results for $[Co(C_2Ph_2)(PMe_3)_3]BPh_4$ were included as well for comparison, this structure being considered here as a distorted square pyramid with an apical PMe_3 ligand, the two remaining PMe_3 molecules and the two central carbon atoms of diphenylacetylene spanning the four basal sites. The square-pyramidal d^6 complex $RuCl_2(PPh_3)_3$ in Table IV possesses an axial Ru–P bond significantly shorter than the basal ones. On the other hand, in the d^8 species $[Co(CNPh)_5]^+$,[11] $[Ni(CN)_5]^{3-}$,[12] and $Ni(CN)_2(P)_3$ (where P = 5-methyl-5*H*-dibenzophosphole),[13] the axial M–L distance is longer than the basal ones. This is in agreement with theoretical calculations for five-coordinate d^6 and d^8 complexes. One can predict a lengthening of the axial M–L bond between a d^6 and a d^8 square-pyramidal complex, the additional electrons going into the d_{z^2} antibonding orbital, thus weakening the axial M–L bond compared to the basal ones.[14] Although the short axial Co–P bond might suggest that $[Co(C_2Ph_2)(PMe_3)_3]BPh_4$ could be envisaged as a d^6 Co(III) species, the roughly equivalent axial and basal Co–P distances show that $[Co(\eta^4\text{-}C_4H_6)(PMe_3)_3]BPh_4$ is definitely on the d^8 Co(I) side (π-bonding).

The Co–C distances in $[(\eta^4\text{-}C_4H_6)(PMe_3)_3]BPh_4$ (average 2.07 Å, Table II) are on the high side of the range obtained for complexes of Co(I) and Fe(0) with π-donor ligands: 2.026 Å (average) in $[Co(C_2H_4)(MeCN)(PMe_3)_3]BPh_4$, 1.979 Å (average) in $[Co(C_2Ph_2)(MeCN)(PMe_3)_3]BPh_4$, 2.10 Å (average) in $Fe(\eta^4\text{-}C_4H_6)(CO)_3$,[15] and 2.12 Å (average) in $Fe(\eta^4\text{-}C_4H_6)_2(CO)$,[16] thus indicating that butadiene behaves as a conventional η^4-diene ligand (π bonding). However, such a geometric criterion has to be handled with caution, since the structure of the different complexes (Table IV) present variations in the square-pyramidal structure. For instance, the metal, which is always above the basal plane, shows a distance to this plane ranging from 0.34 Å in $[Co(CN)_5]^{3-}$ to 0.61 Å in $Fe(C_4H_6)_2(CO)$.

The butadiene ligand is cis and nearly symmetrically positioned about the P(13)–Co–C(X) plane, C(X) being the middle of the C(2)–C(3) bond. The double bonds C(1)–C(2) and C(3)–C(4) are oriented roughly parallel to this plane, which has been predicted to be the best orientation of ethylene in a square pyramid.[14] The ligand is planar within 0.3σ (0.004 Å), and its plane is inclined at an angle of 84.5° to the basal plane. The pattern of the C–C bond lengths (1.44–1.48–1.42 Å, σ = 0.02 Å) is similar to those found in a number of other butadiene complexes.[16,17] Thus, all C–C bonds exhibit partial multiple bond char-

---

[10] La Placa, S. J.; Ibers, J. A. *Inorg. Chem.* **1965**, *4*, 778–783.

[11] Brown, L. D.; Greig, D. R.; Raymond, K. N. *Inorg. Chem.* **1975**, *14*, 645–649.

[12] Raymond, K. N.; Corfield, P. W. R.; Ibers, J. A. *Inorg. Chem.* **1968**, *7*, 1362–1372.

[13] Powell, H. M.; Watkin, D. J.; Wilford, J. B. *J. Chem. Soc. A* **1971**, 1803–1810.

[14] Rossi, A. R.; Hoffmann, R. *Inorg. Chem.* **1975**, *14*, 365–374.

[15] Mills, O. S.; Robinson, G. *Acta Crystallogr.* **1963**, *16*, 758–761.

[16] Whiting D. A. *Cryst. Struct. Commun.* **1972**, *1*, 379–381.

[17] Stephens, F. S. *J. Chem. Soc. A* **1970**, 2745–2748. Van Soest, T. C.; Van der Ent, A.; Royers, E. C. *Cryst. Struct. Commun.* **1973**, *2*, 527–529. Huttner, G.; Neugebauer, D.; Razavi, A. *Angew. Chem., Int. Ed. Engl.* **1975**, *14*, 352–353. Skell, P. S.; McGlinchey, M. J. *Angew. Chem., Int. Ed. Engl.* **1975**, *14*, 195–199. Immirzi, A.; Allegra, G. *Acta Crystallogr., Sect. B: Struct. Crystallogr. Cryst. Chem.* **1969**, *B25*, 120–124. Bassi, I. W.; Scordamaglia, R. *J. Organomet. Chem.* **1972**, *37*, 353–359. Campbell, I. L. C.; Stephens, F. S. *J. Chem. Soc., Dalton Trans.* **1974**, 923–926.

Table I. Fractional Coordinates (×10^4, Co × 10^5) and Equivalent Temperature Factors (×10^3)[b]

atom	*x*	*y*	*z*	U_{eq},[c] Å^2	atom	*x*	*y*	*z*	U_{eq},[c] Å^2
Co(1)	51701 (4)	12895 (9)	8918 (5)	44	C(122)	4032 (3)	277 (7)	1048 (4)	50
Co(2)	20891 (9)	74259 (14)	64167 (8)	157	C(123)	4235 (3)	−337 (8)	1088 (5)	70
Co(3)	15327 (8)	17603 (21)	37920 (10)	155	C(124)	4464 (3)	−597 (8)	1514 (6)	98
P(11)	5228 (1)	1323 (2)	1573 (1)	52	C(125)	4489 (3)	−270 (8)	1881 (5)	78
P(12)	5314 (1)	2626 (2)	899 (1)	55	C(126)	4265 (3)	375 (9)	1811 (5)	80
P(13)	5616 (1)	624 (2)	1013 (1)	58	C(131)	3425 (3)	1320 (8)	935 (4)	60
P(21)	1803 (1)	6412 (2)	5970 (1)	86	C(132)	3281 (3)	567 (9)	811 (4)	64
P(22)	2502 (2)	7396 (5)	6483 (3)	82	C(133)	2968 (3)	443 (11)	487 (5)	102
P(23)	2421 (2)	7780 (5)	6077 (3)	68	C(134)	2780 (4)	1100 (13)	247 (5)	131
P(24)	1873 (2)	8449 (4)	6312 (3)	112	C(135)	2910 (4)	1888 (12)	355 (6)	129
P(25)	1880 (2)	8587 (5)	5876 (3)	68	C(136)	3216 (3)	1983 (10)	678 (5)	85
P(31)	1634 (2)	919 (4)	3377 (2)	175	C(141)	3987 (3)	2304 (8)	1257 (4)	57
P(32)	984 (1)	1473 (3)	3447 (2)	106	C(142)	4230 (3)	2757 (9)	1613 (5)	75
P(33)	1606 (3)	1067 (6)	4307 (4)	286	C(143)	4398 (3)	3402 (8)	1549 (6)	94
C(1)	4863 (3)	244 (8)	757 (5)	82	C(144)	4340 (4)	3566 (8)	1142 (6)	105
C(2)	4675 (3)	1009 (9)	611 (4)	88	C(145)	4119 (5)	3141 (10)	787 (6)	127
C(3)	4756 (3)	1486 (8)	307 (4)	84	C(146)	3936 (4)	2527 (10)	835 (5)	96
C(4)	4997 (3)	1152 (9)	210 (4)	84	C(211)	2869 (3)	1789 (7)	3311 (4)	53
C(5)	2053 (4)	6808 (10)	6932 (5)	101	C(212)	3067 (3)	1426 (8)	3170 (4)	64
C(6)	2291 (6)	7585 (16)	7126 (8)	195	C(213)	2979 (3)	782 (9)	2880 (5)	82
C(7A)	1809 (8)	8326 (20)	6789 (10)	103	C(214)	2695 (4)	434 (7)	2723 (4)	76
C(7B)	2627 (7)	7292 (19)	7090 (10)	92	C(215)	2468 (3)	731 (8)	2854 (4)	76
C(8A)[a]	1685	7804	6425	127	C(216)	2565 (3)	1384 (7)	3146 (4)	62
C(8B)[a]	2488	6755	6779	127	C(221)	3117 (3)	1988 (7)	4157 (4)	46
C(9)	1612 (7)	2607 (18)	3360 (9)	186	C(222)	2934 (3)	1728 (8)	4341 (4)	62
C(10)	1365 (6)	3044 (16)	3489 (8)	160	C(223)	3050 (3)	1215 (8)	4721 (4)	72
C(11)	1491 (7)	2963 (19)	3872 (9)	186	C(224)	3371 (3)	944 (8)	4932 (4)	76
C(12)	1883 (6)	2494 (18)	4088 (9)	176	C(225)	3558 (3)	1174 (8)	4770 (4)	73
C(13)	1975 (6)	2308 (17)	3757 (9)	171	C(226)	3430 (3)	1662 (8)	4378 (4)	69
C(20)	5354 (4)	325 (8)	1870 (5)	84	C(231)	2671 (3)	3136 (7)	3621 (4)	52
C(21)	5530 (3)	2018 (9)	2022 (4)	77	C(232)	2419 (3)	3345 (8)	3205 (5)	73
C(22)	4853 (3)	1534 (9)	1604 (5)	80	C(233)	2187 (4)	3900 (9)	3137 (5)	93
C(23)	5734 (3)	2918 (8)	1244 (5)	86	C(234)	2173 (3)	4297 (9)	3462 (5)	92
C(24)	5256 (4)	3056 (8)	367 (5)	93	C(235)	2400 (4)	4139 (8)	3868 (5)	87
C(25)	5071 (3)	3376 (7)	1012 (4)	58	C(236)	2660 (3)	3553 (8)	3952 (4)	67
C(26)	5764 (4)	790 (11)	603 (5)	103	C(241)	3239 (3)	3163 (7)	3679 (5)	69
C(27)	5992 (3)	757 (9)	1545 (4)	79	C(242)	3486 (3)	3507 (7)	4057 (4)	61
C(28)	5583 (3)	−558 (7)	976 (4)	70	C(243)	3700 (3)	4104 (10)	4063 (5)	100
C(29)	1993 (4)	5405 (12)	6085 (6)	137	C(244)	3672 (3)	4385 (9)	3622 (6)	114
C(30)	1676 (4)	6435 (9)	5391 (5)	94	C(245)	3442 (4)	4081 (9)	3271 (6)	106
C(31)	1418 (5)	6111 (14)	5955 (7)	170	C(246)	3214 (4)	3436 (8)	3275 (5)	86
C(32)	2688 (5)	6652 (13)	6884 (7)	34	C(311)	551 (3)	2331 (8)	1619 (5)	72
C(33)	2754 (7)	8398 (19)	6635 (10)	95	C(312)	881 (4)	2461 (8)	1755 (4)	84
C(34)	2583 (5)	6932 (13)	5978 (7)	37	C(313)	1083 (4)	3024 (10)	2077 (5)	114
C(35)	2167 (6)	8329 (14)	5530 (8)	48	C(314)	933 (5)	3443 (9)	2236 (5)	115
C(36)	2770 (6)	8389 (16)	6349 (8)	67	C(315)	623 (5)	3369 (9)	2161 (5)	113
C(37)	1569 (7)	8171 (18)	6476 (9)	83	C(316)	433 (4)	2789 (8)	1829 (4)	90
C(38)	1517 (7)	8663 (18)	5738 (9)	87	C(321)	469 (3)	1403 (6)	894 (4)	46
C(39)	2080 (6)	9508 (16)	6463 (8)	63	C(322)	610 (3)	1984 (7)	737 (4)	61
C(40)	1460 (7)	8742 (18)	5476 (9)	85	C(323)	696 (3)	1794 (8)	411 (5)	76
C(41)	2005 (7)	9584 (19)	6126 (10)	93	C(324)	635 (3)	1049 (8)	192 (4)	65
C(42)	2080 (7)	8674 (18)	5601 (9)	82	C(325)	492 (3)	436 (8)	324 (4)	70
C(43)	2097 (5)	481 (12)	3709 (6)	145	C(326)	429 (3)	636 (8)	685 (4)	66
C(44)	1603 (4)	1170 (12)	2830 (6)	139	C(331)	387 (3)	764 (7)	1562 (4)	53
C(45)	1397 (5)	−124 (12)	3144 (6)	147	C(332)	189 (3)	568 (8)	1736 (5)	78
C(46)	745 (4)	2220 (12)	3593 (6)	133	C(333)	228 (4)	−74 (9)	2025 (5)	94
C(47)	798 (5)	1521 (13)	2805 (7)	152	C(334)	494 (4)	−549 (8)	2194 (4)	90
C(48)	835 (5)	477 (13)	3605 (7)	163	C(335)	723 (4)	−397 (8)	2066 (4)	83
C(49)	1470 (5)	1216 (12)	4664 (6)	154	C(336)	664 (3)	273 (8)	1741 (4)	72
C(50)	1639 (5)	−157 (13)	4339 (7)	173	C(341)	−37 (3)	1820 (8)	917 (4)	62
C(51)	2038 (5)	1195 (14)	4765 (7)	188	C(342)	−263 (3)	1196 (8)	722 (4)	54
C(111)	3724 (3)	1647 (7)	1764 (3)	40	C(343)	−568 (3)	1427 (9)	433 (5)	82
C(112)	3689 (3)	2416 (7)	1898 (4)	55	C(344)	−676 (3)	2263 (9)	318 (4)	70
C(113)	3612 (3)	2523 (8)	2254 (4)	71	C(345)	−461 (3)	2830 (8)	509 (4)	66
C(114)	3544 (3)	1832 (10)	2436 (4)	74	C(346)	−138 (3)	2652 (8)	827 (4)	64
C(115)	3570 (3)	1022 (8)	2303 (4)	63	B(1)	3792 (3)	1482 (8)	1352 (5)	42
C(116)	3660 (3)	982 (8)	1993 (4)	62	B(2)	2984 (4)	2505 (9)	3709 (5)	54
C(121)	4023 (3)	691 (7)	1388 (4)	48	B(3)	347 (4)	1567 (8)	1242 (5)	56

[a] Fixed at the position obtained by interpolation on the Fourier map with B = 10. Å^2. [b] Phenyl C atoms in BPh_4^- ions are assigned symbols of the type C(*ijk*), where *i* is the same as for the corresponding B atom, *j* is the ring (1–4), and *k* identifies each ring atom (*k* = 1 for the C atom attached to B and the remaining ring carbons are numbered sequentially). [c] U_{eq} $(U_{11} + U_{22} + U_{33} + 2U_{13} \cos \beta)/3$.

acter, as expected for conjugated diolefins. The overall molecular geometry of this complex closely ressembles that of the related iron tricarbonyl species,[15] a result which could be expected on the basis of the analogy of fragments $Fe(CO)_3$ and $[Co(PMe_3)_3]^+$, which both have 14 electrons in their valence shell.

Cation 2. In this case, the molecular structure is basically the same as in type 1 cations, with Co(2)–P(21) being

Table II. Interatomic Distances (Å) in the Ordered $[Co(C_4H_6)(PMe_3)_3]^+$ Cation 1

Co(1)–P(11)	2.214 (4)	C(2)–C(3)	1.48 (2)
Co(1)–P(12)	2.229 (4)	C(3)–C(4)	1.42 (2)
Co(1)–P(13)	2.192 (5)	P(11)–C(20)	1.825 (13)
Co(1)–C(1)	2.100 (14)	P(11)–C(21)	1.869 (14)
Co(1)–C(2)	2.083 (16)	P(11)–C(22)	1.836 (17)
Co(1)–C(3)	2.031 (14)	P(12)–C(23)	1.798 (17)
Co(1)–C(4)	2.081 (13)	P(12)–C(24)	1.839 (16)
Co(1)–X(12)[a]	1.963	P(12)–C(25)	1.813 (15)
Co(1)–X(23)[a]	1.920	P(13)–C(26)	1.856 (17)
Co(1)–X(34)[a]	1.930	P(13)–C(27)	1.836 (14)
C(1)–C(2)	1.44 (2)	P(13)–C(28)	1.889 (12)

[a] X(*ij*) refers to the middle of the C(*i*)–C(*j*) bond in butadiene.

Table III. Bond Angles (deg) in the Ordered $[Co(C_4H_6)(PMe_3)_3]^+$ Cation 1

P(11)–Co(1)–P(12)	94.7 (2)	Co(1)–P(11)–C(21)	122.8 (5)
P(11)–Co(1)–P(13)	100.8 (2)	Co(1)–P(11)–C(22)	115.3 (5)
P(11)–Co(1)–C(1)	88.6 (4)	C(20)–P(11)–C(21)	98.3 (7)
P(11)–Co(1)–C(2)	92.2 (4)	C(20)–P(11)–C(22)	107.9 (7)
P(11)–Co(1)–C(3)	127.6 (4)	C(21)–P(11)–C(22)	102.0 (7)
P(11)–Co(1)–C(4)	165.4 (4)	Co(1)–P(12)–C(23)	118.8 (5)
P(12)–Co(1)–P(13)	101.9 (2)	Co(1)–P(12)–C(24)	116.4 (6)
P(12)–Co(1)–C(1)	158.5 (4)	Co(1)–P(12)–C(25)	114.5 (5)
P(12)–Co(1)–C(2)	118.2 (4)	C(23)–P(12)–C(24)	98.6 (7)
P(12)–Co(1)–C(3)	90.2 (4)	C(23)–P(12)–C(25)	106.7 (7)
P(12)–Co(1)–C(4)	93.8 (4)	C(24)–P(12)–C(25)	99.0 (7)
P(13)–Co(1)–C(1)	98.3 (4)	Co(1)–P(13)–C(26)	116.9 (6)
P(13)–Co(1)–C(2)	136.7 (4)	Co(1)–P(13)–C(27)	120.1 (5)
P(13)–Co(1)–C(3)	129.0 (4)	Co(1)–P(13)–C(28)	115.5 (5)
P(13)–Co(1)–C(4)	89.1 (4)	C(26)–P(13)–C(27)	101.9 (7)
C(1)–Co(1)–C(2)	40.4 (6)	C(26)–P(13)–C(28)	98.0 (7)
C(2)–Co(1)–C(3)	42.0 (6)	C(27)–P(13)–C(28)	101.0 (6)
C(3)–Co(1)–C(4)	40.4 (6)	C(1)–C(2)–C(3)	111.0 (13)
Co(1)–P(11)–C(20)	114.1 (5)	C(2)–C(3)–C(4)	118.1 (13)

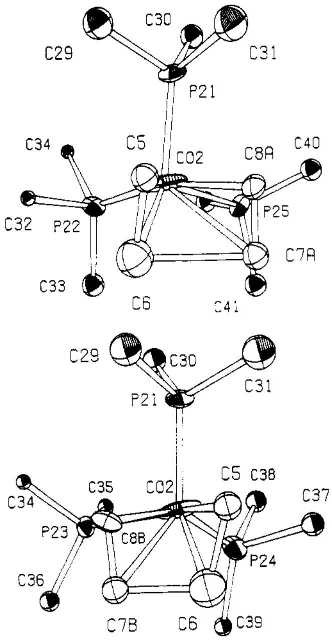

Figure 3. ORTEP drawings of the two disordered individuals for the cation of type 2. Ellipsoids correspond to 30% probability.

the apical bond of the approximate square pyramid (Figure 3). However, the cation occupies the cavity in the BPh_4^- framework in two orientations related by by a ~45° rotation about the apical bond. Although Co(2) was not found in two resolved locations, its positions in these two orientations undoubtedly differ appreciably, as suggested by the elongated thermal ellipsoid. The angles (Table IIIA, supplementary material) still correspond to a square pyramid. However, no great significance should be ascribed to the differences in the Co–P bond lengths (Table IIA, supplementary material), since the individual positions of Co(2) are not known. Furthermore, the refined positions of P(22) and P(24) are probably affected by the proximity of C(8A) and C(8B) in the other image. Nevertheless, the connectivity is clearly established in both individuals and the structure closely resembles that of type 1 cations.

Cation 3. For this cation, the disorder is of a different type (Figure 4). No image duplication was found for the $Co(PMe_3)_3$ unit, but the atomic temperature factors were very high, which probably means that the fragment occupies two individual positions close together. Five regions of electron density around Co(3) were assigned to C atoms of butadiene. In order to group them into individual C_4 units of reasonable geometry, it had to be assumed that three of these positions were approximately coincident in both individuals, while one terminal carbon in each individual would not be overlapping with an atomic site in the other individual. It was hoped that the evolution of the temperature factors during refinement would make it possible to identify the two half-carbon atoms. Unfortunately, all atoms refined with high temperature factors, probably because the positions common to both individuals are only approximately coincident. The two patterns shown in Figure 4 were assembled by inspection of the C–C distances and C–C–C angles, as well as the nonbonded contacts with the $Co(PMe_3)_3$ unit.

Table IV. Comparison of the Geometry of d^8 and d^6 Square-Pyramidal Complexes[a]

	$[Co(CNPh)_5]^+$ ref 11	$[Ni(CN)_5]^{3-}$ ref 12	$[Ni(CN)_2P_3]$[b] ref 13	$[RuCl_2(PPh_3)_3]$ ref 10	$[Co(C_2Ph_2)(PMe_3)_3]^+$ ref 2	$[Co(C_4H_6)(PMe_3)_3]^+$ this work	$FeCO(C_4H_6)_2$ ref 16	$Fe(CO)_3(C_4H_6)$ ref 15
M–L_a, Å	1.88 (3) (C)	2.17 (1) (C)	2.321 (2) (P)	2.230 (8) (P)	2.127 (2) (P)	2.192 (5) (P)	1.94 (2) (C)	1.74 (1) (CO)
M–L_b (av), Å	1.83 (2) (C)	1.86 (1) (C)	2.179 (2) (P)	2.393 (6) (P)	2.212 (2) (P)	2.221 (4) (P)	2.00 (mid ||)	1.77 (1) (CO)
			1.856 (9) (C)	2.388 (7) (Cl)	1.851 (5) (C)	1.95 (mid ||)		1.97 (mid ||)
L_b–M–L_b (av), deg	156.5 (10) (C, C)	159.5 (5) (C, C)	161.2 (1) (P, P)	156.4 (2) (P, P)	136.9 (1) (P, C)	147.5 (P, mid ||)	144.8 (||, ||)	145.9 (C, mid ||)
			140.4 (4) (C, C)	157.2 (2) (Cl, Cl)	137.8 (2) (P, C)	138.4 (P, mid ||)		
L_b–M–L_a (av), deg	101.9 (11)	100.2 (5)	104.6 (3)	101.3 (2)	105.1 (2)	107.3	107.6	106.0
basal plane, deg	0.37	0.34	0.49	0.46	0.47	0.60	0.61	0.50

[a] L_a = apical ligand; L_b = basal ligand. In the C_4H_6 complexes, the middle of each double bond (mid ||) is used to define a corner of the basal plane.
[b] P = 5-Methyl- and 5-ethyl-5*H*-dibenzophosphole.

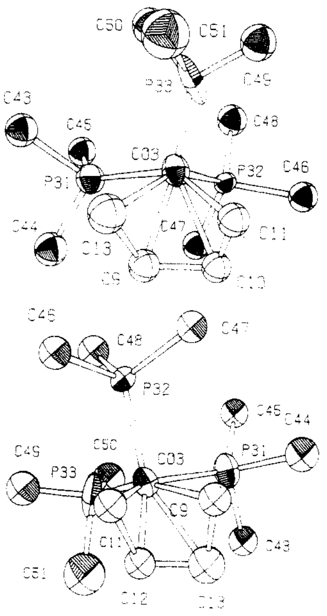

Figure 4. ORTEP drawings of the two disordered individuals for the cation of type 3. Ellipsoids correspond to 30% probability.

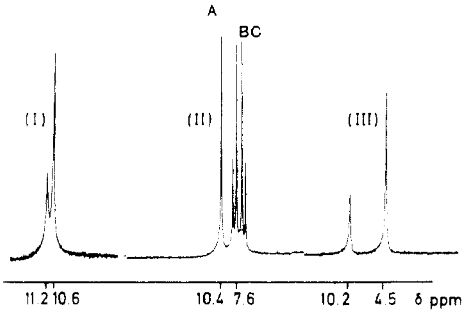

Figure 5. $^{31}P\{^1H\}$ NMR spectra of CD_2Cl_2/CH_2Cl_2 (1/1) solutions of $[Co(\eta^4\text{-}C_4H_6)(PMe_3)_3]BPh_4$ (I) at 183 K, $[Co(\eta^4\text{-}C_5H_8)(PMe_3)_3]BPh_4$, (II) at 163 K, and $[Co(\eta^4\text{-}C_6H_{10})(PMe_3)_3]BPh_4$ (III) at 183 K.

Interestingly, the two isomeric forms of Figure 4 are related by a rotation of 120° of the butadiene ligand about the pseudo-threefold axis of the $Co(PMe_3)_3$ unit. Isomeric forms of this type have been proposed to explain the fluxional behavior of similar compounds,[18-20] and the possibility that the $[Co(\eta^4\text{-}C_4H_6)(PMe_3)_3]^+$ cation be fluxional in the crystal is not unrealistic.

Additional Comments on the Structure. The coordinated PMe_3 molecules show the expected geometry in ordered cation 1, the P–C distances average 1.84 Å, and the C–P–C angles (average 101.5°) are significantly smaller than 109.5° as usual.[2] Similarly, the BPh_4^- ions show no unusual features. The B–C bond lengths average 1.64 Å, and the usual pattern of internal angles is observed: C(ortho)–C(B)–C(ortho) = 113.6°, C(B)–C(ortho)–C(meta) = 123.7°, others = 119.5°.

NMR Studies. The temperature-dependent NMR studies show that the three complexes are stereorigid at low temperature and become fluxional when the temperature increases. The NMR data are reported in Table V and on Figure 5.

The $^{31}P\{^1H\}$ NMR spectrum of I in CD_2Cl_2 at 183 K (Figure 5) shows two broad resonances ($\Delta\nu$ = 18 Hz) in 1:2 ratio at 11.2 and 10.6 ppm without fine structure. Thus, I contains in solution two equivalent basal P_b and a unique apical P_a. This is in agreement with the square-pyramidal structure observed in the solid state. The broadness of the signals precludes the observation of the P_aP_b coupling constant, which is expected to be small in a square-pyramidal d^8 species.[21] In the related $Fe(\eta^4\text{-}C_4H_6)(PMe_2Ph)_3$ complex, a $J_{P_aP_b}$ value of 3 Hz has been reported.[22] Complex III presents a similar AB_2 spectrum (Figure 5), but complex II shows at 163 K an ABC spectrum characterized by a singlet (A) and a quadruplet (BC) in a 1:2 ratio. The singlet at 10.4 ppm results from the resonance of the unique apical phosphorus, while the two basal P atoms display a BC spectrum ($\delta(P_B)$ 6.9; $\delta(P_C)$ 8.2; $J_{P_BP_C}$ = 60 Hz). Thus, the two basal phosphines are magnetically unequivalent at low temperature in the isoprene complex, the only compound containing an unsymmetrical diene.

Scheme I

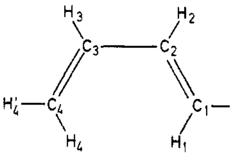

In the low-temperature ^1H NMR spectra of the PMe_3 methyl groups, resonances in a 1:2 ratio are observed in the range 1.2–1.7 ppm for the apical and the basal PMe_3 ligands. The presence of a doublet for the apical methyl group is due to coupling with P_a (J_{HP_a} = 8 Hz), whereas the basal methyl protons are present either as a pseudotriplet (coupling with two basal P_b) or a broad singlet. The $^{13}C\{^1H\}$ NMR spectra (Figure 6 in supplementary material and Table V) also contains two sets of methyl signals for PMe_3 in the range 18–20 ppm for complexes I and III: a triplet for the basal methyl groups coupled with the two basal P_b atoms (J_{CP_b} = 15 Hz) and a doublet for the apical methyl groups coupled with the apical P_a atom (J_{CP_a} = 28 Hz). However, complex II shows, besides the singlet at 20 ppm corresponding to the isoprene methyl group, three doublets for the three magnetically unequivalent PMe_3 ligands. The doublet at about 19.5 ppm (J_{CP} = 26 Hz) corresponds to the CH_3 groups of the apical PMe_3 ligand, which appears at low field compared with the basal PMe_3 groups (Table V). The basal PMe_3 are present as two doublets of doublets (δ 18.2, J_{CP} = 21 Hz, J_{CPP} = 4 Hz, and δ 17.1, J_{CP} = 20 Hz, J_{CPP} = 4 Hz) indicating long-range C–P–P coupling.

Signals attributable to the protons of coordinated dienes (Scheme I) are observed as broad singlets between −0.4 and 0.1 ppm for H1/H4, 1.6 and 1.7 ppm for H1′/H4′, and 4.9 and 5.4 ppm for H2/H3. Coupling constants with neighboring protons have been determined for the butadiene complex I by selective irradiation (Table V). Coupling of H1/H4 (inner hydrogens) with phosphorus is also apparent. The $^{13}C\{^1H\}$ NMR spectra show the magnetic equivalence of the terminal C1 and C4 carbons (with sp^2 hybridization) in the three complexes at low temperature, together with their coupling with the phosphorus atoms. This coupling undoubtedly occurs through the cobalt center, thus indicating the presence of a C1(C4)–Co–P interaction. This type of ^1H and ^{13}C coupling pattern has been observed for several *cis*-butadiene complexes of transition metals, and it is consistent with a normal π interaction. The X-ray work also points to this same

---

(18) Kruczynski, L.; Takats, J. *Inorg. Chem.* **1976**, *15*, 3140–3147.

(19) Van-Catledge, F. A., Ittel, S. D.; Jesson, J. P. *J. Organomet. Chem.* **1979**, *168*, C25–C29; *J. Am. Chem. Soc.* **1979**, *101*, 3874–3884.

(20) Albright, T. A.; Hofmann, P.; Hoffmann, R. *J. Am. Chem. Soc.* **1977**, *99*, 7546–7557.

(21) DuBois, D. L.; Meek, D. W. *Inorg. Chem.* **1976**, *15*, 3076–3083.

(22) Komiya, S.; Minato, H.; Ikariya, T.; Yamamoto, T.; Yamamoto, A. *J. Organomet. Chem.* **1983**, *254*, 83–88.

Table V. ^1H, ^{13}C, and ^{31}P NMR Data (ppm)[a]

$[Co(\eta^4\text{-}C_4H_6)(PMe_3)_3]BPh_4$ (I)	^1H	293 K	0.1 (br) H1, H4; 1.6, 1.8 (br) PMe_3; 1.9 (br) H1′, H4′; 5.6 (br) H2, H3; 6.2 (t), 7.1 (t), 7.5 (br) BPh_4
	^1H	187 K	0.1 (br) H1, H4; 1.4 (m), 1.66 (d, J_{PH} = 8 Hz) PMe_3; 1.7 (br) H1′, H4′; 5.4 (br) H2, H3; $J_{H1-H1'}$ = 2 Hz; J_{H1-H2} = 7 Hz; $J_{H1'-H2}$ = 4 Hz; J_{H2-H3} = 2 Hz; 6.8 (t), 6.9 (t), 7.3 (br) BPh_4
	^{13}C	223 K	18.6 (t, J_{CP} = 15 Hz; J_{CPP} = 4 Hz) CH_3 basal; 20.3 (d, J_{CP} = 28 Hz) CH_3 apical; 40.4 (m, J_{CH} = 158 Hz) C1, C4; 89 (s, J_{CH} = 172 Hz) C2, C3; 121, 125, 135 (J_{CH} = 156 Hz), 164 (q, J_{CB} = 49 Hz) BPh_4
	$^{31}P\{^1H\}$	183 K	10.6 (br) $2P_b$; 11.2 (br) P_a
$[Co(\eta^4\text{-}C_5H_8)(PMe_3)_3]BPh_4$ (II)	^1H	298 K	−0.3 (br), −0.2 (br) H1, H4; 1.3, 1.5 (br) PMe_3; 1.7 (br) H1′, H4′; 2.1 (s) CH_3; 4.9 (m), H3; 6.8 (t), 7.0 (t), 7.3 (br) BPh_4
	^1H	183 K	−0.4 (d, J_{H4-H3} = 8 Hz) H4; −0.3 (s) H1; 1.2 (m), 1.5 (d, J_{PH} = 8 Hz) PMe_3; 1.6 (br) H1′, H4′; 2.5 (s) CH_3; 4.9 (br) H_3; 6.9 (t), 7.0 (t), 7.2 (br) BPh_4
	^{13}C	299 K	19.7 (br) PMe_3; 21 (q, J_{CH} = 127 Hz) C5; 40.5 (t, J_{CH} = 150 Hz) C4; 41.4 (t, J_{CH} = 157 Hz) C1; 89 (d, J_{CH} = 170 Hz) C3; 104.6 (s) C2; 122, 126, 136 (J_{CH} = 157 Hz), 164 (J_{CB} = 50 Hz) BPh_4
	$^{13}C\{^1H\}$	193 K	17.1 (dd, J_{CP} = 20 Hz, J_{CPP} = 4 Hz) CH_3 basal; 18.2 (dd, J_{CP} = 21 Hz, J_{CPP} = 4 Hz) CH_3 basal; 19.5 (d, J_{CP} = 26 Hz) CH_3 apical; 20.0 (s) C_5 (CH_3 isoprene); 39.5 (m) C1, C4; 87.5 (s) C3; 102.5 (s) C2; 120.6, 124, 134, 162 BPh_4
	$^{31}P\{^1H\}$	298 K	3.9 (br) $2P_b$; 6.7 (br) P_a
		163 K	6.9, 8.2 (q, $J_{P_b-P_b}$ = 60 Hz) PMe_3 basal; 10.4 (s), PMe_3 apical
$[Co(\eta^4\text{-}C_6H_{10})(PMe_3)_3]BPh_4$ (III)	^1H	298 K	−0.4 (br) H1, H4; 1.3 (br) PMe_3 basal; 1.5 (br) PMe_3 apical; 1.6 (br) H1′, H4′; 2.0 CH_3; 6.9 (t), 7.0 (t), 7.3 (br) BPh_4
	^1H	183 K	−0.5 (d, J_{HP} = 16 Hz); 1.2 (br) PMe_3 basal; 1.45 (d, J_{HP} = 7 Hz) PMe_3 apical; 1.55 (br) H1′, H4′; 2.0 (s), CH_3; 6.9 (t), 7.0 (6), 7.2 (br) BPh_4
	^{13}C	299 K	19.3 (q, J_{CH} = 127 Hz) C5, C6; 20.0 (q, J_{CH} = 127 Hz) PMe_3; 43.3 (t, J_{CH} = 153 Hz) C1, C4; 102 (s) C2, C3; 121.8, 125.7, 136 (d, J_{CH} = 155 Hz), 164 (q, J_{CB} = 50 Hz) BPh_4
	$^{13}C\{^1H\}$	193 K	18.9 (m), C5, C6, PMe_3 basal; 19.7 (d, J_{CP} = 27 Hz) PMe_3 apical; 42.8 (s), C1, C4; 100.6 (s) C2, C3; 121.4, 125.3, 134.8 (s), 163 (q, J_{CB} = 50 Hz) BPh_4
	$^{31}P\{^1H\}$	298 K	1.7 (br) $2P_b$; 7.6 (br) P_a
		183 K	4.5 (s) $2P_b$; 10.2 (s) P_a

[a] s = singlet, d = doublet, t = triplet, q = quadruplet, br = broad, m = multiplet.

Scheme II

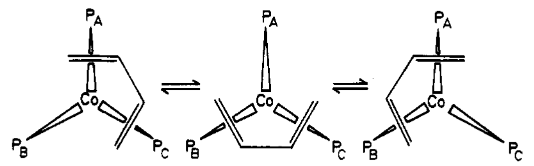

conclusion, since no special shortening of the Co–C1(C4) distance is apparent.

When the temperature is raised the sharp $^{31}P\{^1H\}$ signals for P_a and P_b of I and III gradually broaden, indicating an exchange between the two sites. The broadness of the spectra at room temperature indicates that the coalescence has not yet been reached. We have not further investigated this behavior since in Co complexes, the broadening of the ^{31}P NMR signal occurring at room temperature is due not only to coalescence but also to the ^{31}P–^{59}Co spin–spin interaction resulting from the quadrupolar moment of the Co nucleus.[23,24]

Figure 7 (supplementary material) shows the temperature dependence of the $^{31}P\{^1H\}$ NMR spectrum of complex II. The simplest mechanism, which implies simultaneous exchange between the three P sites, is shown in Scheme II. It is in agreement with the mechanism previously reported for $M(\eta^4\text{-}C_4H_6)L_3$ complexes and is supported here by the X-ray structure determination of I.

Conclusion

X-ray and NMR experiments show that the present cobalt complexes are conventional η^4-diene species and not polydendate η^3-allyl compounds with σ-CH_2 ligand-cobalt interaction, which could in principle result from internal oxidative addition of the diene to the electron-rich Co(I) complex containing only σ-donor PMe_3 ligands. Comparison with the related d^8 ML_3 (butadiene) complexes (M = Fe, Co; L = CO, PR_3, $P(OR)_3$) shows a very similar geometry and stereochemistry for all the complexes.

The X-ray work on $[Co(\eta^4\text{-}C_4H_6)(PMe_3)_3]BPh_4$ shows that the BPh_4^- anions create a framework in which large cavities accommodate the square-pyramidal $[Co(\eta^4\text{-}C_4H_6)(PMe_3)_3]^+$ cations. In one-third of these cavities, the cation is ordered. In a second set of cavities, two isomeric square-pyramidal forms are trapped, which are related by a rotation of 120° of the butadiene ligand about the pseudo C_3 axis of the $Co(PMe_3)_3$ fragment. This result (*i*) gives support to the pathway proposed to explain the fluxional behavior of these species and (ii) suggests that the cation could also be fluxional in the crystal.

We are currently investigating the chemical reactivity of these complexes.

Acknowledgment. We wish to thank Mr. Comminges for running the NMR spectra, M. J. Olivier for collecting the X-ray data, and Prof. J. Takats for helpful comments concerning fluxionality in diene complexes. This work was made possibly by travel grants in the framework of the Programme d'Échanges Universitaires Franco-québécois. Financial support through the Natural Science and Engineering Research Council of Canada and the Ministère de l'Éducation du Québec, the Conselho National de Desenvolvimento Cientifico e Tecnologico CNPq (Brasil) (LCAC), and the Centre National de la Recherche Scientifique (France) is gratefully acknowledged.

Registry No. I, 65836-17-1; II, 65836-19-3; III, 98104-57-5; Co-Br$(PMe_3)_3$, 53432-07-8; butadiene, 106-99-0; isoprene, 78-79-5; 2,3-dimethylbutadiene, 513-81-5.

Supplementary Material Available: $^{13}C\{^1H\}$ NMR spectrum of $[Co(\eta^4\text{-}C_4H_6)(PMe_3)_3]BPh_4$ (Figure 6), variable-temperature $^{31}P\{^1H\}$ NMR spectrum of $[Co(\eta^4\text{-}C_5H_8)(PMe_3)_3]BPh_4$ (Figure 7),

---

(23) Jesson, J. P.; Meakin, P. *J. Am. Chem. Soc.* **1974**, *96*, 5760–5774.

(24) Fellmann, J. D.; Garrou, P. E.; Withers, H. P.; Seyferth, D.; Traficante, D. D. *Organometallics* **1983**, *2*, 818–825.

2028 *Organometallics* **1985**, *4*, 2028-2032

interatomic distances (Table IIA) and bond angles (Table IIIA) in the disordered $[Co(\eta^4\text{-}C_4H_6)(PMe_3)_3]^+$ cations, refined temperature factors (Table VI), calculated coordinates of the hydrogens atoms of the phenyl rings (Table VII), geometry of the BPh_4^- ions (Table VIII), weighted least-squares planes (Table IX), and observed and calculated structure factor amplitudes (Table X) (65 pages). Ordering information is given on any current masthead page.

Triptycene π Complexes. Molecular Structures of $(C_{20}H_{14})Cr(CO)_3$ and $(C_{20}H_{14})Co_4(CO)_9$

Roman A. Gancarz,[1a,b] John F. Blount,[1c] and Kurt Mislow*[1a]

Department of Chemistry, Princeton University, Princeton, New Jersey 08544, and Chemical Research Department, Hoffmann-La Roche, Inc., Nutley, New Jersey 07110

Received March 5, 1985

The crystal and molecular structures of tricarbonyl(η^6-triptycene)chromium (1) and nonacarbonyl(η^6-triptycene)tetracobalt (2) have been determined. Crystals of 1 are monoclinic, space group $P2_1/c$ (no. 14), with a = 13.590 (1) Å, b = 13.403 (3) Å, c = 10.286 (1) Å, β = 109.18 (1)°, and Z = 4. Crystals of 2 are monoclinic, space group $C2/c$ (no. 15), with a = 31.033 (6) Å, b = 14.467 (1) Å, c = 12.183 (1) Å, β = 93.03 (1)°, and Z = 8. Deformations in the molecular structures are consistent with the operation of a steric effect involving nonbonded repulsion between one of the triptycene rings and the $Cr(CO)_3$ and $Co_4(CO)_9$ tripods. Because of the greater steric demand of $Co_4(CO)_9$, the observed effect is markedly more pronounced in 2 than in 1.

Transition-metal π complexes of bulky arenes exhibit stereochemical features of exceptional interest; examples are the conformational variability in chromium complexes of hexaethylbenzene[2] and restricted rotation about the arene-metal bond in a ruthenium complex of 1,4-di-*tert*-butylbenzene.[3] Some years ago, Pohl and Willeford[4] suggested the possibility of restricted rotation about the benzene–chromium bond in tricarbonyl(η^6-triptycene)chromium (1) but noted that the barrier to rotation "could be reduced considerably, either by a tilting of the tricarbonylchromium with respect to the plane of the ring to which it is bonded, or by significant distortion of the triptycene molecule itself". The present work was undertaken in order to determine whether such distortions have a significant effect on the ground-state structure of 1.[5] In addition we also determined the structure of nonacarbonyl(η^6-triptycene)tetracobalt (2), a compound in which the deformations described by Pohl and Willeford are expected to be substantially more severe. Prior to the present work, no X-ray structures of triptycene π complexes had been reported.

Experimental Section

Infrared spectra were recorded on a FTS-20C Digilab FT-IR spectrometer. ^1H NMR spectra were recorded on a Bruker WM 250 spectrometer. All reported chemical shifts are reported in parts per million downfield relative to tetramethylsilane. Reagents were obtained from Strem Chemicals (dicobalt octacarbonyl and chromium hexacarbonyl) and Aldrich (triptycene). Hexane, pentane, and benzene were distilled from sodium-benzophenone and purged with argon before reaction. All reactions were carried out in an inert (argon) atmosphere.

Tricarbonyl(η^6-triptycene)chromium (1) was prepared as described previously.[4] The product was purified by column chromatography on neutral alumina, eluting first with hexane, to remove triptycene, and then with benzene. Crystals suitable for X-ray analysis were grown by layering a concentrated solution of 1 in benzene with an equal volume of hexane and allowing the solutions to diffuse slowly in the dark at room temperature: yellow crystals; mp 232–236 °C dec (lit.[4] mp 235–236 °C dec; lit.[6] mp 237 °C dec); IR (cyclohexane) 1975 (s), 1913 (s) cm^{-1} (lit.[4] 1975, 1910 cm^{-1}; lit.[6] 1974, 1906 cm^{-1}). The ^1H NMR spectrum ($CDCl_3$, ambient temperature) featured an apparent singlet, corresponding to the aliphatic bridgehead protons (δ 5.14 (2 H)), and three pairs of multiplets, corresponding to the AA′ and BB′ portions of the aromatic protons in each of the three rings (and identified as such by decoupling experiments): set 1 (δ 5.04–5.10 (2 H) and 5.66–5.73 (2 H)), set 2 (δ 6.97–7.04 (2 H) and 7.31–7.37 (2 H)), and set 3 (δ 7.07–7.15 (2 H) and 7.37–7.42 (2 H). Pohl and Willeford[4] report a bridgehead singlet at δ 5.18 and two "A_2B_2 patterns" centered at δ 5.40 and 7.28. Moser and Rausch[6] report a bridgehead singlet at δ 5.10, a multiplet for the aromatic protons of the complexed ring centered at δ 5.30, and a multiplet for the aromatic protons of the two uncomplexed rings centered at δ 7.15.

Nonacarbonyl(η^6-triptycene)tetracobalt (2). A solution of triptycene (0.51 g, 2 mmol) and tetracobalt dodecacarbonyl (0.57 g, 1 mmol) in a mixture of dodecane (1.5 mL) and dioxane (1.5 mL) was heated for 8 min at 125–130 °C while a slow stream of argon was maintained through the solution. The solution was cooled, diluted with pentane (10 mL), and chromatographed on Florisil. Elution of the unreacted $Co_4(CO)_{12}$ with hexane (violet band) was followed by elution with 1:1 v/v hexane–benzene and benzene to recover the desired product (green band). The eluate was evaporated, and the residue (0.7–2.1 mg, 0.1–0.3% yield) was dissolved in pentane. Crystals suitable for X-ray analysis were obtained by cooling the pentane solution (containing, if necessary, a small amount of benzene to increase the solubility). The greenish black crystals decompose above 180 °C: IR (cyclohexane) 2068 (m), 2049 (w), 2025 (s), 2004 (m), 1990 (s), 1892 (s), 1885 (s), 1841 (s), 1826 (s). The ^1H NMR spectrum ($CDCl_3$, ambient temperature) featured an apparent singlet, corresponding to the aliphatic

---

[1] (a) Princeton University. (b) On leave of absence from the Technical University, Wrocław, Poland. (c) Hoffmann-La Roche, Inc.

[2] (a) Hunter, G.; Iverson, D. J.; Mislow, K.; Blount, J. F. *J. Am. Chem. Soc.* **1980**, *102*, 5942. (b) Iverson, D. J.; Hunter, G.; Blount, J. F.; Damewood, J. R., Jr.; Mislow, K. *Ibid.* **1981**, *103*, 6073. (c) Hunter, G.; Blount, J. F.; Damewood, J. R., Jr.; Iverson, D. J.; Mislow, K. *Organometallics* **1982**, *1*, 448. (d) Hunter, G.; Wadsworth, W. S., Jr.; Mislow, K. *Ibid.* **1982**, *1*, 968. (e) Blount, J. F.; Hunter, G.; Mislow, K. *J. Chem. Soc., Chem. Commun.* **1984**, 170.

[3] Pomeroy, R. K.; Harrison, D. J. *J. Chem. Soc., Chem. Commun.* **1980**, 661.

[4] Pohl, R. L.; Willeford, B. R. *J. Organomet. Chem.* **1970**, *23*, C45.

[5] Professor Willeford kindly encouraged us to proceed with this work since his own intended X-ray study of 1[4] had failed to materialize (Willeford, B. R., private communication).

[6] Moser, G. A.; Rausch, M. D. *Synth. React. Inorg. Met.-Org. Chem.* **1974**, *4*, 37.

0276-7333/85/2304-2028$01.50/0